Heliyon

Received:
16 October 2018
Revised:
30 January 2019
Accepted:
18 March 2019

Cite as: Feras Alshehri, Víctor García Suárez, José L. Rueda Torres, Arcadio Perilla, M. A. M. M. van der Meijden. Modelling and evaluation of PEM hydrogen technologies for frequency ancillary services in future multi-energy sustainable power systems. Heliyon 5 (2019) e01396.
doi: 10.1016/j.heliyon.2019.e01396

Modelling and evaluation of PEM hydrogen technologies for frequency ancillary services in future multi-energy sustainable power systems

Feras Alshehri [a], **Víctor García Suárez** [a], **José L. Rueda Torres** [a,*], **Arcadio Perilla** [a], **M. A. M. M. van der Meijden** [a,b]

[a] *Department of Electrical Sustainable Energy, Delft University of Technology, Mekelweg 4, 2628 CD, Delft, the Netherlands*

[b] *TenneT TSO B. V, Arnhem, the Netherlands*

[*] Corresponding author.

E-mail address: j.l.ruedatorres@tudelft.nl (J.L. Rueda Torres).

Abstract

This paper examines the prospect of PEM (Proton Exchange Membrane) electrolyzers and fuel cells to partake in European electrical ancillary services markets. First, the current framework of ancillary services is reviewed and discussed, emphasizing the ongoing European harmonization plans for future frequency balancing markets. Next, the technical characteristics of PEM hydrogen technologies and their potential uses within the electrical power system are discussed to evaluate their adequacy to the requirements of ancillary services markets. Last, a case study based on a realistic representation of the transmission grid in the north of the Netherlands for the year 2030 is presented. The main goal of this case study is to ascertain the effectiveness of PEM electrolyzers and fuel cells for the provision of primary frequency reserves. Dynamic generic models suitable for grid simulations are developed for both technologies, including the required controllers to enable participation in ancillary services markets. The obtained results show that PEM hydrogen technologies can

https://doi.org/10.1016/j.heliyon.2019.e01396

improve the frequency response when compared to the procurement with synchronous generators of the same reserve value. Moreover, the fast dynamics of PEM electrolyzers and fuel cells can help mitigate the negative effects attributed to the reduction of inertia in the system.

Keyword: Electrical engineering

1. Introduction

Hydrogen is viewed as one the most important drivers of the progressive decarbonization of the transportation, industrial and electricity sectors. The global demand of hydrogen is already on the rise, and it is expected to significantly increase in future years. By 2025, the total consumption is predicted to reach 50 million tons [1]. By 2050, the most optimistic predictions foresee that hydrogen will constitute 18% of the final total energy demand [2]. The synergy between the electricity and gas sectors (i.e. power-to-gas) has gained popularity over the last years due to the different opportunities that multi-energy conversion can offer. Principally, water electrolysis technology allows the exploitation of the surplus generation from renewable energy sources to produce green hydrogen. By carrying the energy in the form of molecules instead of electrons, long-term energy storage is enabled. Large quantities of hydrogen can be stored in underground salt caverns, to be used later as feedstock for industrial consumers, fuel cell electric vehicles and fuel cell electricity generation [3]. Furthermore, hydrogen can be subjected to methanation in order to create synthetic gas (i.e. syngas), a fuel mainly used for electricity generation in gas turbines and for a handful of industrial processes. Syngas can be injected safely into the natural gas network as well, potentially allowing to manage the daily and seasonal electricity demand variations [4]. From all the cited applications, it is clear that the coupling of the electricity and gas sectors is worth studying and evaluating, especially in countries with a strong presence of chemical industrial activity (e.g. Germany) and/or a large generation of electricity with gas fired power plants (e.g. the Netherlands).

For the electrical power system, the reduction of CO_2 emissions is being achieved by gradually substituting traditional thermal synchronous generators with stochastic renewable energy sources. Although the operation of the electrical network in this new scenario is becoming more challenging for Transmission System Operators (TSOs), the future European grid is still expected to be smarter, more robust and more reliable. Flexibility will be the key requirement for the success of this energy transition. Flexible generation, demand side response technologies and multi-energy sector couplings constitute few of the solutions that will help unlock the full potential of the future power system.

https://doi.org/10.1016/j.heliyon.2019.e01396

Particularly for hydrogen technologies, limited research has focused so far on the possibility of procuring electrical ancillary services, which are managed by TSOs to handle contingencies in the power system. This paper aims to contribute to this topic by thoroughly discussing the technical feasibility and adequacy of PEM electrolyzers and fuel cells to partake in future European ancillary services markets. To that end, this research also investigates the development of electrical models for these technologies that are suitable for dynamic stability studies. Finally, the presented case study provides valuable insight into the benefits that the synergy between the electricity and hydrogen sectors can bring to power system stability when applied to frequency regulation.

The remainder of the paper is structured as follows: Section 2 discusses the future framework of European ancillary services markets. Section 3 reviews the latest developments of PEM electrolyzers and fuel cells, explores their potential value for power system operation and details how these technologies are modelled for electrical studies. Section 4 defines the case study and examines the obtained results. Section 5 summarizes the drawn conclusions.

2. Background

Real-time power system operation is challenged on a daily basis by numerous disturbances such as faults, demand alterations or fluctuating renewable energy, which can induce undesired frequency, voltage or congestion issues in the electrical system. Ensuring an effective and reliable grid operation is handled by TSOs, in part, through the procurement of ancillary services.

Traditionally, the framework of ancillary services markets around Europe has been subjected to the specific rules of the corresponding national TSOs [5]. However, as a consequence of frequency variations affecting every control area in the grid regardless of the origin of the disturbance, the development of a single common European frequency balancing market is being pursued for the beginning of the 2020s decade [6]. In such scenario, it is expected that the mitigation of renewable energy uncertainty will be more effective, and at the same time, it will create a harmonized market playing field across Europe in terms of prequalification requirements, contracting procedures, procurement methods and pricing settlement rules.

In this section, the framework of the most promising ancillary services markets for the participation of PEM hydrogen technologies is briefly discussed. The structure of frequency balancing markets holds special importance due to being the main focus of the proposed case study, and it is therefore emphasized.

2.1. Frequency containment reserve (FCR)

Limiting frequency excursions after a sudden imbalance of generation and demand is essential to guarantee the dynamic stability of the power system. For such purpose,

https://doi.org/10.1016/j.heliyon.2019.e01396

FCR (formerly known as primary frequency control) is used. According to ENTSO-E, an overall FCR capacity of ±3000 MW is currently allocated in the interconnected synchronous area of Continental Europe, further divided proportionally between the member states [7]. The FCR market is already partially harmonized, as a total capacity of ±1400 MW is auctioned together in a joint platform, composed by the different TSOs from Germany, the Netherlands, Austria, Switzerland, Belgium and France [8].

The FCR auction takes place once a week, and it allows participation of generators, loads and storage technologies. A single symmetric capacity product is requested (i.e. upward and downward regulation are indivisible), offered in steps of 1 MW and with a minimum bid size of ±1 MW. The product resolution lasts for one entire week, and it is remunerated on a pay-as-bid scheme. Since 2015, FCR prices have progressively declined, mainly due to the increased level of competition associated with the entry of new players in the market (especially battery storage) [7]. In 2018, the average price was 12.75 €/MW/h (roughly a 42% reduction with respect to 2015) [8]. For a hypothetical supplier contracted for all 52 weeks, the annual revenue would have totaled 111 k€/MW.

By 2021, the described market framework will have undergone several modifications [9]. To begin with, Denmark is expected to have joined the market by that point. More importantly, to help integrate renewable energy and decentralized sources, the product duration will be split into 6 daily time slots of 4 hours each. The auction will occur once per day, one day before the actual procurement (D-1). The settlement rule will be changed to marginal pricing, hence probably leading to slightly higher prices. The average price under the marginal clearing rule in 2018 would have been 13.75 €/MW/h (i.e. total annual revenue of 120 k€/MW if contracted for all 52 weeks) [8]. For 2030, the inclusion of other neighboring countries to the common FCR market is an educated guess, which ideally will reach the total capacity of ±3000 MW. The implementation of asymmetric bids is also feasible, as it will further boost the operational freedom of suppliers and allow an optimal use of the available capacity.

In terms of technical requirements, FCR procurement relies on a decentralized linear control able to change the active power output proportionally to the frequency deviation (e.g. droop characteristic) [10]. A maximum deadband of ±10 mHz around 50 Hz may be established in the controller. The activation of the full bid must be completed within 30 seconds for a deviation of ±200 mHz or more. For providers with unlimited energy supply, support must persist until the frequency deviation ceases. In line with the regulatory market changes planned for the next years, it is probable that the technical requirements will become more stringent at some point, either by shortening the full activation time or by incentivizing the participation of faster technologies.

https://doi.org/10.1016/j.heliyon.2019.e01396

2.2. Automatic frequency restoration reserve (aFRR)

The restoration process to bring the frequency back to the nominal value is addressed via aFRR (formerly known as secondary frequency control). Currently, the framework of aFRR in Europe is entirely dependent on national legislation, and so far, only Germany and Austria share a pilot common aFRR market [6]. Nevertheless, all participants in the shared FCR market, plus Denmark and Czech Republic are part of the International Grid Control Cooperation (IGCC) [11], which features advanced technical coordination to prevent different control areas from activating opposite direction aFRR simultaneously.

The required minimum aFRR capacity per country, typically between 3 to 4 times bigger than the one for FCR, is usually guaranteed via the specific capacity product of each territory [5]. The market harmonization plan proposed for Continental Europe for the early 2020s focuses exclusively on an energy product [6], yet the definition of the capacity product, or lack thereof, will still be delegated to the corresponding national authorities. The daily deployment of aFRR will likely be split into 96 periods of 15 minutes each. For each individual period, a European bid ladder will be constructed, with gate closure time one hour before the procurement (H-1). The common ladder will gather both the mandatory bids from the providers contracted for the capacity product and additional free capacity bids from other units. These voluntary bids can be asymmetric, offered in steps of 1 MW and at least 1 MW total in size. When a power imbalance occurs, a common cross-border merit order list will determine the energy activation of the suppliers, prioritizing the cheapest bids and at the same time avoiding possible congestions in the cross-border interconnectors. The last unit that gets activated in the period will determine the cross-border marginal energy price.

For the activation of aFRR, units must follow the setpoints sent by the TSOs from a centralized Load Frequency Control (LFC), as to correctly restore the power balance in all the control areas. It is expected that the full bid activation time will be no more than 5 minutes, indicating a minimum ramp rate of 20% of the bid per minute [6].

The potential of the aFRR market regarding supplier revenue is hard to estimate, as neither imbalances nor the merit order list can be predicted. Taking the Dutch system as reference [12], which probably resembles the structure of the goal European aFRR market the most, the average price of the capacity product in 2017 was approximately 10 €/MW/h (i.e. total annual revenue of 86 k€/MW if contracted for the entire year) [12]. For upward aFRR energy regulation, for which TSOs remunerate suppliers (vice versa for downward regulation), the average settlement price in 2018 was 81 €/MWh during peak hours (i.e. 08:00 to 20:00) and 75 €/MWh during the rest of the day [13].

https://doi.org/10.1016/j.heliyon.2019.e01396

2.3. Voltage control

Since voltage stability is inherently a local issue, each TSO follows its own framework regarding voltage control [5]. National grid codes usually demand mandatory voltage regulation capabilities to synchronous generators and power electronic interfaced renewable energy sources connected to the transmission grid. Other equipment such as transformers, FACTS (Flexible AC Transmission Systems), HVDC (High-Voltage Direct Current) links, battery storage and several industrial consumers are also able to cope with voltage control duties. The optimal use of the reactive power provided by these sources is defined by the TSOs based on optimization programs, past experience and/or grid studies [5]. Supplier remuneration relies on the national legislation as well.

2.4. Congestion management

TSOs can approach different strategies in order to relieve the congestion of transmission lines [12]. For instance, the redispatch of power plants and large demand side response constitutes a widely used local relief action, but it comes at a combined cost of several billions of euros in Europe every year. In Germany alone, the total redispatching costs in 2018 almost reached 1 B€ [14]. TSOs can minimize the call for redispatch and anticipate for future transmission capacity needs by investing in infrastructural upgrades for the grid. On a European level, TSOs can also make use of available cross-border capacity to alleviate congestions [12].

3. Model

Existing research in the field of water electrolysis anticipates that PEM technology will be the industry standard for the year 2030 [15]. In the present day, PEM systems are already available on a commercial level, yet their substantial capital costs constitute the main industry goal moving forward [15, 16]. In comparison to long-established alkaline systems, PEM is favored due to its higher power density, better cell efficiency, improved hydrogen purity and faster dynamic performance [15]. With respect to solid oxide systems, research has showed that although this technology can achieve greater efficiency than PEM [17], its dynamic response for load changes is significantly slower [18, 19], thus limiting the participation in ancillary services that require fast power variations.

The basic internal structure of PEM devices consists of porous electrodes separated by a solid electrolyte layer, a catalyst layer situated between the electrolyte and the electrodes, and an external electrical circuit connected across the electrodes. The electrolyte layer allows the transfer of only hydrogen ions (protons), while the electrons flow through the external circuit. This structure is shown in Fig. 1 for both electrolyzers and fuel cells. In the case of electrolyzers, electrical energy is consumed to

https://doi.org/10.1016/j.heliyon.2019.e01396

decompose water into hydrogen and oxygen molecules. In the case of fuel cells, hydrogen and oxygen molecules are split by the catalyst into atoms and then into ions, releasing electrical energy and forming water molecules. In-depth descriptions of the electrolyzer and fuel cell technology can be found in existing literature [20, 21].

This section serves as an overview of the state of the art of PEM hydrogen technologies, namely electrolyzers and fuel cells. The discussed topics include the latest developments from different manufacturers and future expectations for the year 2030, the potential contribution of these technologies to power system flexibility, the adopted modelling approach for power system dynamic stability studies, and the adequacy to future ancillary services markets.

3.1. PEM electrolyzers

The fundamental business principle behind power-to-gas resides in the exploitation of cheap electricity to produce hydrogen, when the entire process is more cost-effective than the direct purchase of hydrogen on the market [22]. The rate at which hydrogen is produced is proportional to the input DC electrical power. Electrolyzers can generate around 15 kilograms of hydrogen per hour for each installed MW [16], with overall plant efficiency ranging from 70-80% [16], and a maximum lifetime of the electrolysis stack close to 80,000 hours of operation (up to 30 years for the rest of the equipment in the installation) [23]. The maximum size of a single PEM electrolyzer currently sits at 3 MW [24], but larger systems can be constructed by following a modular aggregation of individual units [16]. With regard to the investment costs, the capital expenditure for this technology is currently priced on 1 M€/MW, while the additional yearly operational costs are less than 5% of the initial investment [25]. During the next decade, the capital cost is anticipated to decrease by half due to technology improvements, larger sizes and economies of scale [15, 16]. All in all, the promising prospect of power-to-gas conversion has ignited the development of numerous small-scale electrolyzer demonstration projects around Europe and other

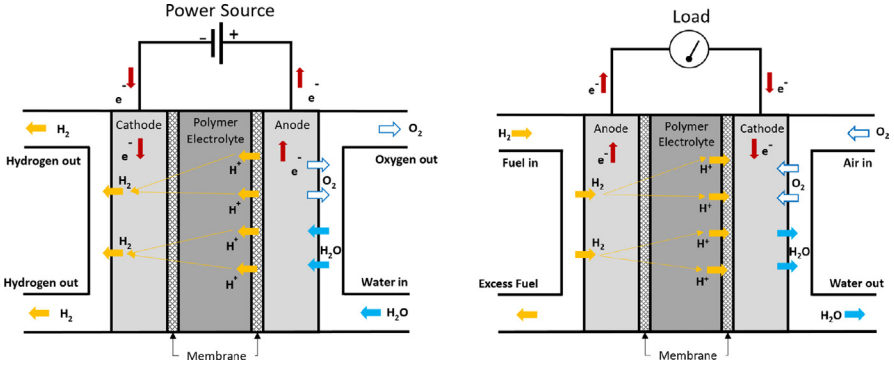

Fig. 1. Schematics of PEM devices: electrolyzer (left) and fuel cell (right).

https://doi.org/10.1016/j.heliyon.2019.e01396

parts of the world. Not only that, but few commercial projects on a larger scale have already been announced, like a 10 MW refinery in Germany [26], and a 13 MW methanation plant in Austria [27]. Others are still on the initial planning stages, as in the case of a potential 20 MW facility for hydrogen mobility in the Netherlands [28].

From the point of view of the electrical network, the most interesting capability of PEM electrolyzers lies in the fast dynamics of the electrolysis process. Ramping up and down to change the consumption of electricity can be completed in less than 1 second [29]. Shutting down can be done within seconds and coming back online can be achieved in a few minutes [25, 29]. Also, partial loading levels with respect to the rated capacity can be sustained during long periods of time [29]. The cited technical characteristics open up several potential demand side response schemes to support the operation of electrical power systems. For instance, fleets of electrolyzers could be coordinated with large renewable energy sources to help mitigate the fluctuations of generated power [29, 30]. Besides, they could be commanded to quickly increase their consumption at times when there is surplus of renewable energy, as to minimize the curtailment of electricity.

For electrical studies, a complete representation of the PEM electrolyzer unit includes the modelling of the stack, the power conversion system (i.e. transformer and electronic converters) and the balance of plant (i.e. electrical consumption of the other equipment of the installation) [31]. The electrolysis stack can be reduced to an equivalent circuit composed by the open circuit DC voltage of the stack, plus a resistor in series to represent the different internal electrical losses. The electrolyzer is coupled to the grid via an AC-DC rectifier, followed by a DC-DC converter that controls the input power by modulating the electrical current.

For power system analysis, the accuracy of the ramping dynamics of the electrolyzer is the most relevant aspect of the modelling process, as it will determine how the frequency response is influenced. As already mentioned, manufacturers guarantee that PEM electrolyzers can vary power consumption within 1 second [16, 23]. However, limited information is publicly published concerning the evolution of the power curve and the definition of more precise settling times. Due to this fact, the electrolyzer model was approximated as an equivalent dynamic load that emulates the performance of the few existing laboratory tests (i.e. settling time within 250 milliseconds) [29].

Additional controllers are implemented to enable the procurement of ancillary services, which would add extra value to the power-to-gas business model by complementing the revenue earned from the sale of hydrogen or syngas [22]. For FCR, the classic droop characteristic is adapted for demand side response technologies, so that electrolyzer consumption is lowered when the frequency drops and increased when the frequency rises. The inverse droop characteristic is implemented by simply

https://doi.org/10.1016/j.heliyon.2019.e01396

changing the minus sign for a plus sign in the droop definition block from the control scheme of the PEM fuel cell, later depicted in Fig. 2. From a market standpoint, PEM electrolyzers show much quicker technical capabilities than the prequalification requirements of FCR. From the year 2021 onwards, the reduced resolution of the FCR product will give electrolyzers more operational flexibility to optimize their bidding strategy. Likewise, for aFRR, the quarter hour periods and the introduction of voluntary bidding will make the provision of upward regulation accessible for electrolyzers.

For steady state voltage control, electrolyzers can provide support when operating at partial load, since the remainder capacity of the AC-DC converter that feeds the stack can be used to inject reactive power to the grid. Also, it is feasible to indirectly influence voltage by varying the active power consumption of the units. Finally, critical peak loads and congestions in transmission lines can be alleviated by curtailing the consumption of electricity, or even by completely interrupting operation. For each service, the variation of the active or reactive power setpoint is managed via an external signal, that simulates a direct request from the TSO.

3.2. PEM fuel cells

The generation of electricity with fuel cells, which uses hydrogen as feedstock, has proved its feasibility for diverse sectors, such as stationary power applications (e.g. telecommunication services, backup power generators), transportation services (e.g.

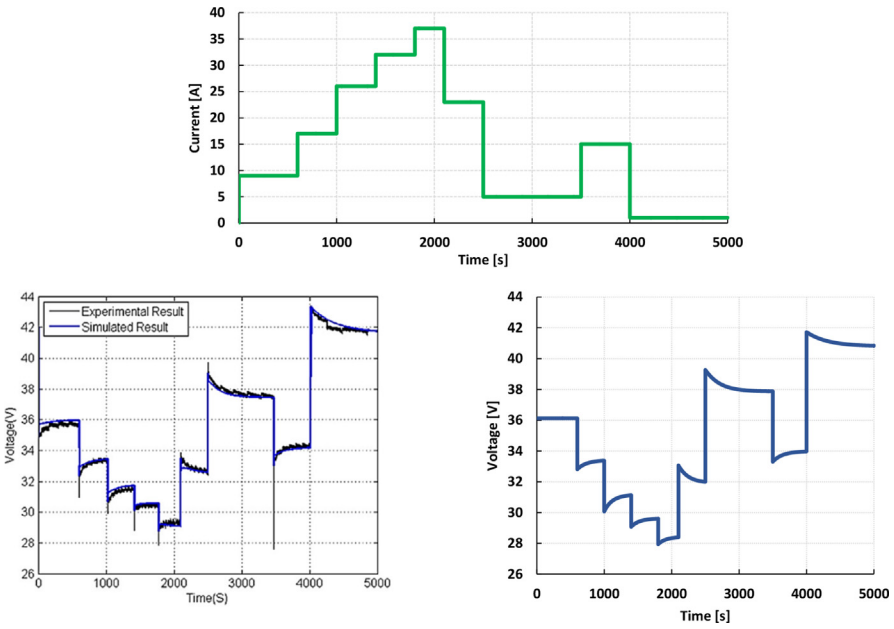

Fig. 2. Validation of the dynamic model of the PEM fuel cell stack: simulated current profile (up), voltage response from literature [49] (bottom left) and voltage response from simulated model (bottom right).

https://doi.org/10.1016/j.heliyon.2019.e01396

buses, cars, material handling vehicles) and portable power applications [32]. PEM technology in particular, raises the most interest for electric vehicles, since it can provide fast time response and high power density [17]. The combination of fuel cells with electrolyzers is also very promising, as it opens the possibility to create a cheap hydrogen supply that can be stored and later used by fuel cells to support the demand of the power grid.

So far, the maximum size for a PEM fuel cell plant is 2 MW [33]. In similar fashion to electrolyzers, multiple units can be operated in parallel to achieve larger capacities. For instance, one of the largest facilities in the world is based on individual 2.8 MW molten carbonate fuel cells, amounting for a total of 59 MW [34]. The reported PEM fuel cell efficiency is in the range of 40−60% according to most sources [17, 35, 36], with an estimated annual capacity factor of 95% [37], and a lifetime rounding the 40,000 hours [37]. The capital cost of PEM fuel cells lies between 1.5 M€/MW to 3 M€/MW [35], with an associated payback period of around 8 years [37]. The high capital cost is due to the elevated price of platinum catalysts [38], which on the other hand can be salvaged after the decommission of the cells. The annual operational cost is less than 1% of the initial investment [35].

In general, fuel cell technology has demonstrated the ability to provide stable and independent electricity to individual consumers [39], to the power grid and even to microgrids [40]. However, very little research has been done to specifically address their potential to participate in electrical ancillary services. For future frequency balancing markets, PEM fuel cells share comparable ramping technical capabilities to electrolyzers, as it is also possible to complete active and reactive power setpoint changes within 1 second [41]. For aFRR, fuel cells could take advantage of the cheap hydrogen supplied by electrolyzers to place voluntary bids for upward regulation during periods with high settlement prices. For voltage support, PEM fuel cells can be more effective than electrolyzers, as the presence of a DC-AC inverter allows complete control over the output power factor. Furthermore, fuel cells can provide additional benefits in the case of distributed generation, where multiple units can participate in local voltage support at different locations in the low voltage network or within a microgrid [40]. Last, large fuel cell plants can contribute to the relief of transmission line congestions via bidirectional power redispatch.

In literature, several approaches have been adopted to develop the model and characterization of the steady state and dynamic behavior of fuel cells. For example, models based on electrochemical equations [42, 43, 44, 45], provide valuable insight into the reactions that occur within the stack, yet they are very complex and require the knowledge of technical parameters that are not publicly available. On the other hand, models based on mathematical approximations, semi-empirical or empirical data and model fitting [46, 47, 48, 49, 50, 51], are usually simpler, but they represent

https://doi.org/10.1016/j.heliyon.2019.e01396

specific commercial fuel cells, and therefore they may not be generalized to all existing units.

For this paper, an electrical depiction of a grid-connected PEM fuel cell was developed, which covers the dynamics of the stack, the power conditioning system (i.e. DC-AC inverter) and the balance of plant. The presented model is built upon previous research [52], that estimates physical parameters through experimentation and empirical data collection from the 1.2 kW (26 V and 46 A) Nexa PEM fuel cell, a frequently studied unit in this field. An advantage of the Nexa model is the inclusion of an air compressor, a cooling fan and fully automated control of the hydrogen flow, air supply and stack temperature [53], making it possible to incorporate the description of the balance of plant within the dynamic equations.

For the modelling of the PEM fuel cell, the following assumptions have also been considered. Supplied hydrogen and air behave as ideal and uniformly distributed gases injected at constant pressure to the gas flow channels of the fuel cell. The thermodynamic properties of the stack are evaluated at the average stack temperature, with constant stack specific heat capacity and for a constant ambient temperature of 25 °C. The parameters of individual fuel cells can be lumped together to represent a single stack, and several stacks can be aggregated to portray a fuel cell plant. Finally, the hydrogen storage capacity is sufficiently large to supply enough hydrogen to the fuel cell and to absorb the hydrogen produced by the electrolyzers.

The set of equations that govern the dynamic behavior of the stack are summarized in Table 1. The output voltage of the fuel cell after a current setpoint change (Eq. 1) [54], is computed as the Nernst potential (Eq. 2) [55], minus the electrical losses produced in the internal resistance of the cell (Eq. 3) and the electrochemical activation losses due to the Tafel slope (Eq. 4). These parameters are dependent on the temperature of the stack (Eq. 5), which is a function of the initial and steady state temperature values after the current modification, both of them determined through curve fitting of the utilized empirical data [53]. This particular fuel cell does not operate in the range where concentration losses become significant and hence, they are not considered [52]. It is also worth noting that the 47 factor in the computation of the Nernst potential accounts for the number of individual cells within the studied stack. The remaining parameters in the equations are also estimated using empirical data fitting [52, 53].

The described equations show that the output voltage of the fuel cell changes almost instantaneously, although it presents an over- or undershoot that decays exponentially over time. Consequently, the output power varies very rapidly as well, but due to the delay in the thermodynamic response of the fuel cell, it does not reach the desired setpoint until minutes later. The developed stack model is validated against available experimental data from literature [49], by measuring the stack voltage after a series of changes in the current drawn by the fuel cell. As observed

https://doi.org/10.1016/j.heliyon.2019.e01396

Table 1. Set of equations that define the dynamic behaviour of the modelled PEM fuel cell stack.

N°	Equation	Variables	Definition	Value	Unit
(1)	$V_{FC} = V_{OC} - V_R - V_A = E_0 - I \cdot R - A \cdot \ln\left(\frac{I}{I_{ex}}\right)$	V_{FC}	Stack voltage		[V]
		E_0	Nerst potential		[V]
		I	Output current		[A]
		R	Internal resistance		[Ω]
		A	Tafel slope		[V]
		I_{ex}	Exchange current	$1 \cdot 10^{-6}$	[A]
(2)	$E_0 = 47 \cdot [1.482 - 0.000845 \cdot T + 0.0000431 \cdot T \cdot \ln(p_{H_2} \cdot p_{O_2}^{0.5})]$	T	Stack temperature		[K]
		p_{H2}	H_2 pressure	1.35	[atm]
		p_{O2}	O_2 pressure	1.00	[atm]
(3)	$R(T) = R_0 \cdot \exp\left(\frac{E_{a,R}}{R_g \cdot T_K}\right)$	R_0	Pre-exponential factor	0.1537	[Ω]
		$E_{a,R}$	Activation energy	1800	[J/mol]
		R_g	Universal gas constant	8.3143	[J/mol•K]
(4)	$A(T) = A_0 \cdot \exp\left(\frac{E_{a,A}}{R_g \cdot T_K}\right)$	A_0	Pre-exponential factor	0.1591	[V]
		$E_{a,A}$	Activation energy	5344	[J/mol]
(5)	$T(t) = T_2 + (T_1 - T_2) \cdot \exp\left(-\frac{H_t}{mc_p} \cdot t\right)$	T_1	Initial temperature		[K]
		T_2	Final temperature		[K]
		H_t	Heat transfer coefficient	$15.07 \cdot I^{0.2358}$	[W/C°]
		mc_p	Heat capacitance	4304	[J/C°]

in Fig. 2, the obtained dynamic response is almost identical to the one of the literature models, with the exception of the inferior voltage measured at low current levels. This issue, which might be caused by the simplification of the model equations, does not affect the reliability of the dynamic model for grid-connected applications, since the fuel cell does not operate outside of its standard power operating range (i.e. $< 20\%$).

Overall, the applied modelling structure allows the decoupling between the fuel cell dynamics on the DC side and the power injection on the AC side, thus enabling the model to be representative of a PEM fuel cell plant of any size. The general frame of the model is illustrated in Fig. 3. The output DC power of the fuel cell is fed into the power conditioning system, which is represented by a PQ controller that generates and forwards the required AC current setpoints to a static generator module. The block diagram of the PQ controller is described in detail in Fig. 4, and it consists of an outer power control loop that controls the active and reactive power, and a faster inner current control loop that controls the d-q axis currents. Each loop has signal filtration and is controlled with a proportional-integral (PI) controller. The static generator is used by the simulation software to represent any non-rotating generator technology connected to the grid via an electronic converter [56].

The initial dynamic response provided by PEM fuel cells is more than sufficient for the procurement of ancillary services. The error between the initial and desired voltage and power values can be overcome by applying corrective control measures to maintain the output power at a constant level while taking into consideration the exponential decay. The control schemes to enable the participation in ancillary

https://doi.org/10.1016/j.heliyon.2019.e01396

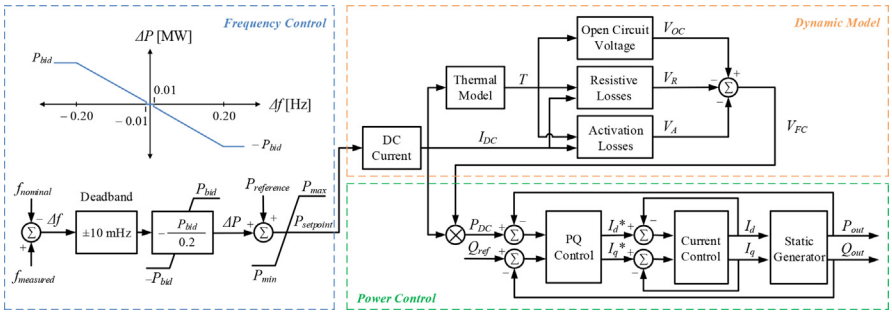

Fig. 3. Dynamic model, control block diagram and droop characteristic of the modelled PEM fuel cell.

services follow almost the same structure as for the electrolyzer. For FCR, a classic droop characteristic is implemented in accordance to the technical requirements of FCR [10]. For voltage control and congestion management, an external reactive or active power setpoint signal is used respectively.

4. Results & discussion

Previous research has pointed out that the integration of a large capacity of PEM electrolyzers in the grid can make a positive contribution to frequency containment [30]. Fuel cells have also demonstrated potential to support frequency when installed in combination with wind turbines [57]. This paper goes a step further, by focusing on how the combined operation of large-scale PEM electrolyzers and fuel cells would influence the frequency performance in different future scenarios.

Before moving on to the specific details, the research methodology used to create this case study is concisely summarized. After validating the electrical models developed for the hydrogen technologies, they are integrated into a realistic test network. A disturbance that affects the balance between generation and demand is induced in the system (e.g. disconnection of generating power) and the subsequent frequency response is measured. This procedure is repeated, varying different parameters such as the capacity of PEM electrolyzers and fuel cells dedicated to frequency control and the level of inertia present in the system. To conclude, the most relevant frequency performance indicators are analyzed to determine the impact of the provision of frequency ancillary services by PEM hydrogen technologies on the stability of the grid.

4.1. Description of the test network

The proposed case study is set in the northern section of the Dutch transmission grid, an area considered to be a promising location for the installation of large-scale power-to-gas capacity in the future due to the abundance of wind parks and the potential for hydrogen storage in underground salt caverns [58]. The modelled system

https://doi.org/10.1016/j.heliyon.2019.e01396

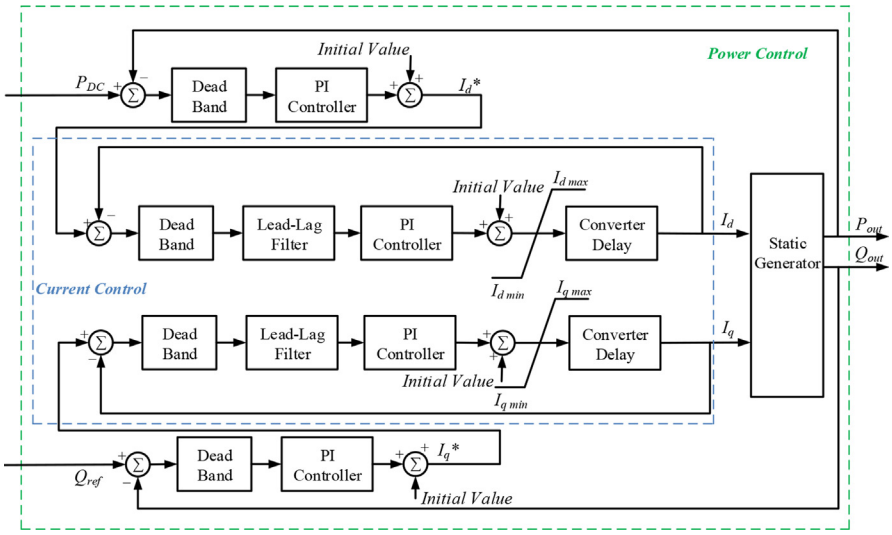

Fig. 4. Power control loops for the modelled PEM fuel cell.

covers the 380 kV and several key connections of the 220 kV high voltage network for the year 2030. The topology of the grid, the power flow conditions and the electricity demand were derived from the guidelines of the ten-year development plan of the Dutch TSO [59].

The test network, depicted in Fig. 5, features a generation capacity composed by two 2250 MVA thermal power plants equipped with two generation units each, 600 MW offshore wind energy (Gemini wind park) and 3058 MW onshore wind energy distributed around the area and further aggregated into the corresponding 380 kV substations. Additional renewable energy is imported via the HVDC interconnectors with Norway (NorNed) and Denmark (COBRAcable), both operated at the rated power transfer capacity of 700 MW. The total installed capacity of PEM electrolyzers and fuel cells amounts to 300 MW and 50 MW respectively, and it is achieved by the aggregation of smaller units. Both facilities operate at a reference power setpoint that allows participation in the future FCR market via symmetrical bidding.

The network was modelled in DIgSILENT PowerFactory, version 2018 SP1. The synchronous generators and the wind turbines were represented by generic models of each technology available in the software. Generic steam turbine-governors with droop control, exciter and power stabilizer were also implemented with the synchronous generators to enable dynamic control and the provision of ancillary services. For this particular study, it was assumed that the wind parks and the HVDC interconnectors did not participate in the regulation of the system. For such reason, the model of the HVDC links was simplified as a constant negative load. The connections to other parts of the network and the local demands were also modelled as constant loads. Due to confidentiality reasons, the parameters of the components of the grid model are not provided.

https://doi.org/10.1016/j.heliyon.2019.e01396

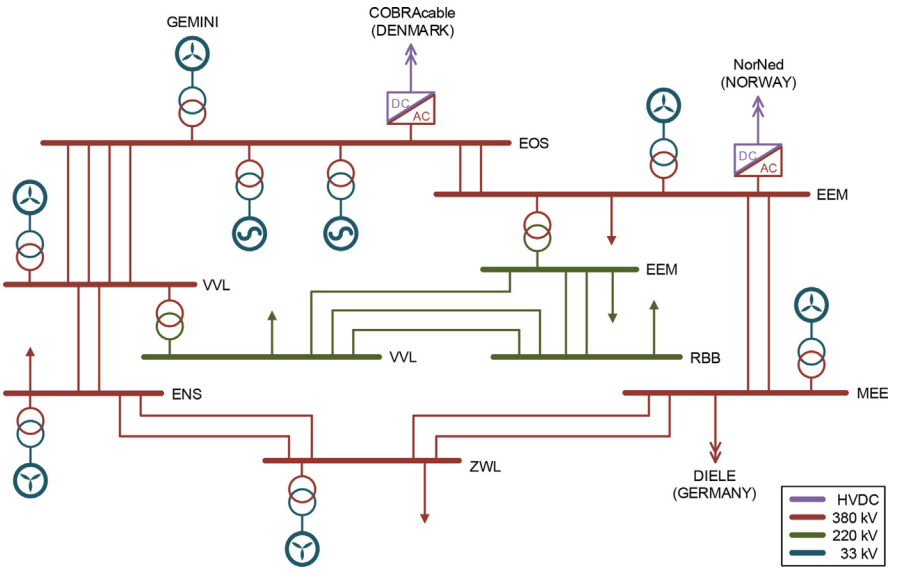

Fig. 5. Single line diagram of the modelled section of the Dutch electrical transmission grid.

The FCR capacity available in the system is set to 50 MW (45% of the total in the Netherlands [8]), while the synchronous generators provide a cumulative rotational inertia of 12 seconds. Both values constitute approximately 1.5% of the total with respect to the entire synchronous area of Continental Europe, and therefore, the proposed model can be considered as a reasonably accurate small-scale grid representation.

4.2. Simulation scenarios and results

The most representative scenarios studied are summarized in Table 2. The network is subjected to a sudden decrease in generation, originated by the disconnection of several wind turbines or by the loss of imported power from the HVDC links. For each of the four scenarios defined, several simulations were performed, varying the location of the disturbance and the distribution of the electrolyzers and fuel cells within the network. Nonetheless, the initial conditions before the event and the amount of generation lost are constant in every case to ensure a fair comparison between the results. The frequency indicators displayed in Table 2 and the frequency responses plotted in Fig. 6 belong to a disturbance occurring at the EEM bus and a location of the PEM hydrogen technologies at the EOS bus.

The first scenario is set as the base case, derived from the current grid conditions. Rotational inertia is very high, there is no presence of PEM electrolyzers or fuel cells and FCR support comes exclusively from the synchronous generators. The second scenario is a hypothetical variation of the base case in which the hydrogen technologies were already installed and providing FCR. By comparing these situations in Fig. 6, it is apparent how the fast dynamics of the PEM hydrogen technologies

https://doi.org/10.1016/j.heliyon.2019.e01396

Table 2. List of scenarios, FCR bid sizes per technology and obtained values of the frequency indicators.

N°	Scenario	System inertia*	Sync. generators	PEM electrolyzer	PEM fuel cell	Nadir [Hz]	RoCoF [mHz/s]
(1)	Base case (2018)	100%	2 × 25 MW FCR bid	Not installed	Not installed	49.851	26.972
(2)	Base case with H_2 (2018)	100%	No FCR support	40 MW FCR bid	10 MW FCR bid	49.902	26.376
(3)	Energy transition (2030)	50%	1 × 25 MW FCR bid	20 MW FCR bid	5 MW FCR bid	49.876	53.882
(4)	Low inertia with H_2 (2050)	25%	No FCR support	40 MW FCR bid	10 MW FCR bid	49.902	99.600

* The value of the system inertia for the base case is 12 seconds.

improve the frequency response. During the first seconds after the disturbance, the frequency drop in both simulations is almost equal, as the inertia of the system is identical. On the other hand, the action of PEM electrolyzers and fuel cells translates into a more linear response and improves considerably the maximum frequency deviation (i.e. frequency nadir). This is attributed to their ability to quickly change the operating setpoint, in contrast to the inherent oscillating behavior of synchronous generators.

The third scenario depicts the energy transition in the power system. Rotational inertia is decreased by half to represent the decrease in synchronous generation over time, the PEM hydrogen technologies are in place and they procure FCR in combination with the synchronous generators. From the results, it can be

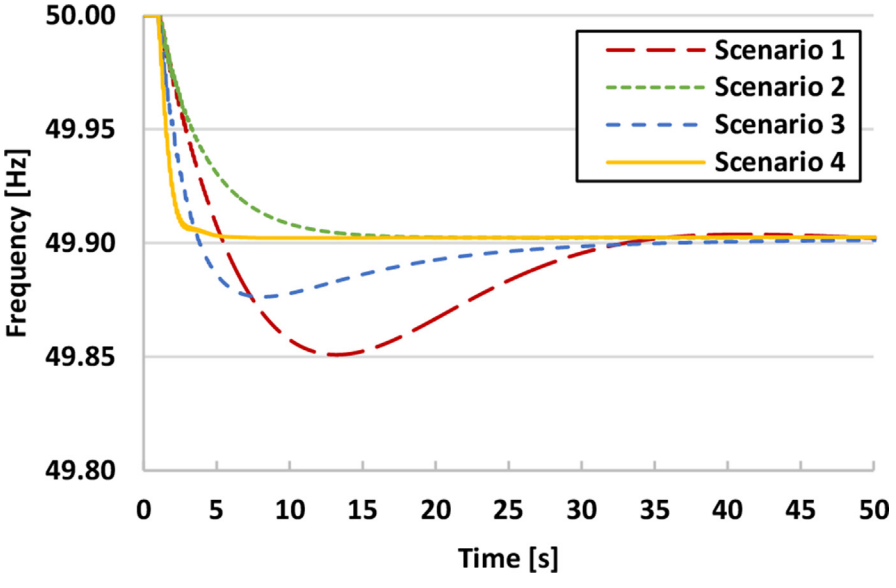

Fig. 6. Frequency response for the described scenarios.

https://doi.org/10.1016/j.heliyon.2019.e01396

observed that the reduction of inertia translates into a steeper slope in the frequency response, technically known as rate of change of frequency (RoCoF). Nevertheless, the inclusion of PEM electrolyzers and fuel cells still improves the value of the frequency nadir with respect to the base case. In the final scenario, it is assumed that most of the thermal generation has been phased out, thus reducing the inertia to a low level. The PEM hydrogen technologies are the only suppliers of FCR. In this case, the frequency drop right after the disturbance is even steeper (around 4 times faster than the base case) because of the lack of dominant inertial behavior. Yet once again, the fast recovery by the PEM electrolyzers and fuel cells is able to limit the frequency nadir to a better value than in the base case.

Furthermore, while keeping the FCR bid size constant, the fast dynamics of PEM electrolyzers and fuel cells could be exploited to enhance the frequency response by increasing the delivered regulation capacity for the same frequency deviations. This can be achieved by modifying the maximum frequency deviation below the default value of ± 0.20 Hz in the control system, which effectively increases the slope of the droop characteristic. The frequency responses for increasingly droop slope values in the low inertia scenario are shown in Fig. 7. As expected, a better steady state value and frequency nadir are accomplished with steeper slopes. Also, the time it takes to reach the nadir is lowered, which indirectly improves the RoCoF, albeit not significantly. However, small oscillations are induced in the system.

During the course of the simulations different disturbance locations were tested, but the aforesaid findings (cf. Table 2 and Fig. 6) did not deviate significantly. Several distributed setups for the PEM hydrogen technologies were examined as well, but it was found that concentrated capacity performs slightly better for frequency regulation. It is worth noting that the used test network is a very strong grid. For weaker grids and more severe disturbances the impact of the distribution and location of the frequency reserve capacity gains importance. Locations of PEM electrolyzers and fuel cells close to critical buses in the network tend to produce an improved dynamic performance [60].

To conclude, the presented case study exemplifies why the participation of PEM hydrogen technologies in the FCR market benefits the frequency stability of the future power system. The decommissioning of traditional power plants will decrease the level of rotational inertia in the grid, which has a negative impact on the robustness of the system against disturbances. Regardless, the introduction of large amounts of flexible and fast technologies (e.g. PEM electrolyzers, PEM fuel cells, battery storage) should be able to strengthen the frequency stability of the system, mainly by limiting the frequency deviations.

https://doi.org/10.1016/j.heliyon.2019.e01396

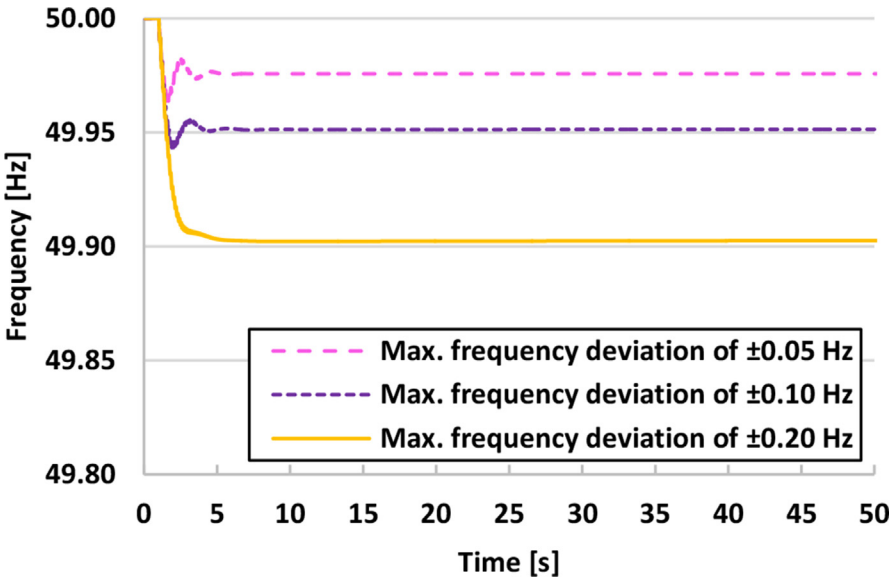

Fig. 7. Frequency response for different droop slopes in the low inertia with H_2 scenario.

5. Conclusions

This paper developed a generic electrical model for grid-connected PEM electrolyzers and fuel cells that is appropriate for power system stability studies and analyzed how these technologies can contribute to the operation of the power system through the procurement of ancillary services.

The comparison of the technical capabilities of PEM electrolyzers and fuel cells with respect to the requirements of future European ancillary services markets, indicated that partaking in frequency regulation, voltage control and congestion management is a feasible option, which can constitute a supplementary source of revenue for the business model of such hydrogen technologies. Concretely, the changes in the framework of balancing markets planned for the coming years are essential to facilitate the integration of PEM electrolyzers and fuel cells in both the FCR and aFRR market.

From the point of view of the electrical power system, the capability of PEM electrolyzers to rapidly change the power consumption and the fast power injection of PEM fuel cells emerges as a very attractive feature for frequency stability. The examined case study, based on realistic projections of the northern Netherlands grid for the year 2030, further highlights the value of PEM hydrogen technologies in the ongoing energy transition. It was observed that the reduction of rotational inertia inevitably causes a detrimental effect in the frequency response during the first seconds after a sudden mismatch between generation and demand. However, when PEM electrolyzers and fuel cells provide FCR support, the frequency deviations can be limited. As a result, better frequency nadir values are obtained than when

https://doi.org/10.1016/j.heliyon.2019.e01396

using traditional synchronous generators, even in the case of minimum system inertia. Further, the ramping requirements of the frequency-power characteristic could be intensified to optimally exploit the capabilities of PEM hydrogen technologies for FCR.

Future research will explore potential methods to attenuate the large RoCoF values caused by the low inertia in the grid. Different control schemes for wind parks and HVDC links will be implemented and tested. Furthermore, in order to improve the overall frequency response, the interaction of such controllers with the presented PEM hydrogen technologies will be analyzed.

Declarations

Author contribution statement

Feras Alshehri, Victor Garcia Suarez, Jose Luis Rueda Torres, Arcadio Perilla, Mart van der Meijden: Performed the experiments; Analyzed and interpreted the data; Wrote the paper.

Funding statement

This work has received funding from Connecting Europe Facility of the European Union, Dutch Ministry of Infrastructure and Environment, and TenneT TSO B.V.

Competing interest statement

The authors declare no conflict of interest.

Additional information

No additional information is available for this paper.

References

[1] CertifHy, Overview of the Market Segmentation for Hydrogen across Potential Customer Groups, Based on Key Application Areas, June, 2015.

[2] Hydrogen Council, Hydrogen Scaling up − A Sustainable Pathway for the Global Energy Transition, Nov. 2017.

[3] J. Töpler, J. Lehmann, Hydrogen and Fuel Cell: Technologies and Market Perspectives, Springer, 2015.

[4] European Power to Gas Platform, Power to Gas − Overview, 2018 [Online]. Available: http://europeanpowertogas.com/power-to-gas/.

https://doi.org/10.1016/j.heliyon.2019.e01396

[5] ENTSO-E, Survey on Ancillary Services Procurement, Balancing Market Design 2017, May 2018 [Online]. Available: https://docstore.entsoe.eu/Documents/Publications/Market%20Committee%20publications/ENTSO-E_AS_survey_2017.pdf.

[6] ENTSO-E, Consultation on the Design of the Platform for Automatic Frequency Restoration Reserve (aFRR) of PICASSO Region, Nov. 2017.

[7] TenneT TSO B.V., Market Review 2016 – Electricity Market Insights, Arnhem, the Netherlands, Mar. 2017 [Online]. Available: https://www.tennet.eu/fileadmin/user_upload/Company/Publications/Technical_Publications/Dutch/2016_Market_Review_TenneT.pdf.

[8] regelleistung.net, Internetplattform zur Vergabe von Regelleistung, 2018 [Online]. Available: https://www.regelleistung.net.

[9] ENTSO-E, "TSOs' Proposal for the Establishment of Common and Harmonised Rules and Processes for the Exchange and Procurement of Balancing Capacity for Frequency Containment Reserves (FCR) in Accordance with Article 33 of Commission Regulation (EU) 2017/2195 Establishing a Guideline on Electricity Balancing," Apr. 2018.

[10] TenneT TSO B.V., Productspecificatie FCR, Nov. 2015 [Online]. Available: https://www.tennet.eu/fileadmin/user_upload/Bijlage_B_-_Productspecifications_FCR_ENG.pdf.

[11] ENTSO-E, Imbalance Netting, 2018 [Online]. Available: https://www.entsoe.eu/major-projects/network-code-implementation/electricity-balancing/igcc/Pages/default.aspx.

[12] TenneT TSO B.V., Market Review 2017 – Electricity Market Insights, Arnhem, the Netherlands, Mar. 2018 [Online]. Available: https://www.tennet.eu/fileadmin/user_upload/Company/Publications/Technical_Publications/Dutch/2017_TenneT_Market_Review.pdf.

[13] TenneT TSO B.V, Settlement Prices, 2018 [Online]. Available: http://www.tennet.org/english/operational_management/System_data_relating_processing/settlement_prices/index.aspx.

[14] ENTSO-E, Costs of Congestion Management, 2018 [Online]. Available: https://transparency.entsoe.eu/congestion-management/r2/costs/show.

[15] O. Schmidt, et al., Future cost and performance of water electrolysis: an expert elicitation study, Int. J. Hydrogen Energy 42 (52) (Nov. 2017) 30470–30492.

https://doi.org/10.1016/j.heliyon.2019.e01396

[16] ITM Power, Scaling PEM Electrolysis to 100 MW, Hannover Messe, Germany, Apr. 2017 [Online]. Available: https://www.h2fc-fair.com/hm17/images/forum/tf/2017-04-25-1100.pdf.

[17] A. Alaswad, et al., Fuel cell technologies, applications, and state of the art. A reference guide, in: Reference Module in Materials Science and Materials Engineering, 2016.

[18] J. Milewski, J. Lewandowski, "Comparative analysis of time constants in Solid Oxide Fuel Cell processes − selection of key processes for modeling power systems, Journal of Power Technologies 91 (1) (2011) 1−5.

[19] N. Zhou, et al., Modelling and control of solid oxide fuel cell generation system in microgrid, J. Electr. Eng. 68 (6) (2017) 405−414.

[20] R.B. Gupta, Hydrogen Fuel: Production, Transport, and Storage, CRC Press, 2008.

[21] P. Breeze, The proton exchange membrane fuel cell, Fuel Cells (2017) 33−43. Academic Press.

[22] J. Eichmann, A. Townsend, M. Melaina, Economic Assessment of Hydrogen Technologies Participating in California Electricity Markets, National Renewable Energy Laboratory, Denver, CO, Feb. 2016. Technical Report NREL/TP-5400-65856.

[23] Siemens, Silyzer 200 Electrolyzer, Nuremberg, Germany, May 2017 [Online]. Available: https://www.siemens.com/content/dam/webassetpool/mam/tag-siemens-com/smdb/corporate-core/sustainable_energy/hydrogensolutions/brosch%C3%BCren/silyzer200-broschure-en.pdf.

[24] Hydrogenics, Hydrogenics Unveils 3 Megawatt PEM Electrolyzer Stack, 2017 [Online]. Available: http://www.hydrogenics.com/2017/04/25/hydrogenics-unveils-3-megawatt-pem-electrolyzer-stack/.

[25] J. de Bucy, The Potential of Power-To-Gas, ENEA Consulting, Paris, France, Jan. 2016.

[26] ITM Power, World's Largest Hydrogen Electrolysis in Shell's Rhineland Refinery, 2018 [Online]. Available: http://www.itm-power.com/news-item/worlds-largest-hydrogen-electrolysis-in-shells-rhineland-refinery.

[27] McPhy, Power-to-Gas in Austria, 2017 [Online]. Available: http://mcphy.com/en/press-releases/power-to-gas-in-austria/.

[28] AkzoNobel, AkzoNobel and Gasunie Looking to Convert Water into green Hydrogen Using Sustainable Electricity, 2018 [Online]. Available: https://

https://doi.org/10.1016/j.heliyon.2019.e01396

www.akzonobel.com/for-media/media-releases-and-features/akzonobel-and-gasunie-looking-convert-water-green-hydrogen.

[29] J. Eichmann, K. Harrison, M. Peters, Novel Electrolyzer Applications: Providing More than Just Hydrogen, National Renewable Energy Laboratory, Denver, CO, Sep. 2014. Technical Report NREL/TP-5400-61758.

[30] V. García, et al., Integration of power-to-gas conversion into Dutch electrical ancillary services markets, in: ENERDAY 2018 – 12th Conference on Energy Economics and Technology, Dresden, Germany, Apr. 2018.

[31] P. Ayivor, et al., Modelling of large size electrolyzer for electrical grid stability studies in real time digital simulation, in: 3rd International Hybrid Power Systems Workshop, Tenerife, Spain, May 2018.

[32] S. Curtin, J. Gangi, Fuel Cell Technologies Market Report 2016, Fuel Cell and Hydrogen Energy Association, Washington, D.C., Oct. 2017. DOE/EE-1672.

[33] S. Barrett, Dutch Partners Deliver First 2 MW PEM Fuel Cell Plant in China, 2017 [Online]. Available: http://www.renewableenergyfocus.com/view/45502/dutch-partners-deliver-first-2-mw-pem-fuel-cell-plant-in-china/.

[34] POWER Magazine, 59-MW Fuel Cell Park Opening Heralds Robust Global Technology Future, 2014 [Online]. Available: http://www.powermag.com/59-mw-fuel-cell-park-opening-heralds-robust-global-technology-future/.

[35] S. Mekhilef, R. Saidur, A. Safari, Comparative study of different fuel cell technologies, Renew. Sustain. Energy Rev. 16 (1) (Jan. 2012) 981–989.

[36] S.J. Peighambardoust, S. Rowshanzamir, M. Amjadi, Review of the proton exchange membranes for fuel cell applications, Int. J. Hydrogen Energy 35 (17) (Sep. 2010) 9349–9384.

[37] V. Das, et al., Recent advances and challenges of fuel cell based power system architectures and control – a review, Renew. Sustain. Energy Rev. 73 (Jan. 2017) 10–18.

[38] P.C. Ghosh, High platinum cost: obstacle or blessing for commercialization of low-temperature fuel cell technologies, Clean Technol. Environ. Policy 19 (2) (Mar. 2017) 595–601.

[39] S. Curtin, J. Gangi, State of the States: Fuel Cells in America 2016, Fuel Cell Technologies Office, U.S. Department of Energy, Nov. 2016.

[40] S. Morozumi, Micro-grid demonstration projects in Japan, in: 2007 Power Conversion Conference - Nagoya, Nagoya, 2007, pp. 635–642.

https://doi.org/10.1016/j.heliyon.2019.e01396

[41] K. Nikiforow, et al., "Power ramp rate capabilities of a 5 kW proton exchange membrane fuel cell system with discrete ejector control, J. Power Sources 381 (Mar. 2018) 30−37.

[42] J.C. Amphlett, et al., A model predicting transient responses of proton exchange membrane fuel cells, J. Power Sources 61 (1) (July 1996) 183−188.

[43] C. Wang, M.H. Nehrir, S.R. Shaw, Dynamic models and model validation for PEM fuel cells using electrical circuits, IEEE Trans. Energy Convers. 20 (2) (June 2005) 442−451.

[44] J. Andujar, F. Segura, M. Vasallo, "A suitable model plant for control of the set fuel cell − DC/DC converter, Renew. Energy 33 (4) (Apr. 2008) 813−826.

[45] I. San Martín, A. Ursúa, P. Sanchis, Modelling of PEM fuel cell performance: steady-state and dynamic experimental validation, Energies 7 (2) (Feb. 2014) 670−700.

[46] Y. Hou, Z. Yang, G. Wan, An improved dynamic voltage model of PEM fuel cell stack, Int. J. Hydrogen Energy 35 (20) (Oct. 2010) 11154−11160.

[47] X. Kong, A.M. Khambadkone, S.K. Thum, A hybrid model with combined steady-state and dynamic characteristics of PEMFC fuel cell stack, in: Industry Applications Conference, 2005. Fourtieth IAS Annual Meeting. Conference Record of the 2005 3, Oct. 2005, pp. 1618−1625.

[48] M.V. Moreira, G.E. da Silva, A practical model for evaluating the performance of proton exchange membrane fuel cells, Renew. Energy 34 (7) (July 2009) 1734−1741.

[49] M. Soltani, S.M.T. Bathaee, Development of an empirical dynamic model for a Nexa PEM fuel cell power module, Energy Convers. Manag. 51 (12) (Dec. 2010) 2492−2500.

[50] C. Restrepo, et al., Identification of a proton-exchange membrane fuel cell's model parameters by means of an evolution strategy, IEEE Transactions on Industrial Informatics 11 (2) (Apr. 2015) 548−559.

[51] P. Gabrielli, et al., Modeling for optimal operation of PEM fuel cells and electrolyzers, in: Environment and Electrical Engineering (EEEIC), 2016 IEEE 16th International Conference, June 2016.

[52] H. Kim, et al., A simple dynamic model for polymer electrolyte membrane fuel cell (PEMFC) power modules: parameter estimation and model prediction, Int. J. Hydrogen Energy 35 (8) (Apr. 2010) 3656−3663.

https://doi.org/10.1016/j.heliyon.2019.e01396

[53] Ballard Power Systems Inc, NexaTM Power Module User's Manual MAN5100078, June 2003 [Online]. Available: http://my.fit.edu/~swood/Fuel%20Cell%20Manual.pdf.

[54] J. Laramie, A. Dicks, Fuel Cell Systems Explained, John Wiley and Sons, New York, 2003.

[55] R. O'hayre, et al., Fuel Cell Fundamentals, John Wiley & Sons, 2016.

[56] DIgSILENT GmbH, DIgSILENT PowerFactory 2016 User Manual, DIgSILENT GmbH, Gomaringen, Germany, Mar. 2016.

[57] J. Morren, S.W. De Haan, J. Ferreira, Primary power/frequency control with wind turbines and fuel cells, in: Power Engineering Society General Meeting, 2006, IEEE, 2006, p. 8.

[58] TSO 2020, TSO 2020: Electric "Transmission and Storage Options" along TEN-E and TEN-T Corridors for 2020, 2018 [Online]. Available: http://tso2020.eu/.

[59] TenneT TSO B.V., Samenvatting KCD 2017, Arnhem, the Netherlands, 2017 [Online]. Available: https://www.tennet.eu/fileadmin/user_upload/Company/Publications/Technical_Publications/Dutch/TenneT_KCD2017_samenvatting.pdf.

[60] V. García, et al., Demand side response in multi-energy sustainable systems to support power system stability, in: 16th Wind Integration Workshop, Berlin, Germany, Oct. 2017.

https://doi.org/10.1016/j.heliyon.2019.e01396